# Quantitative annular dark field scanning transmission electron microscopy for nanoparticle atom-counting: What are the limits?

**A De Backer[1], A De wael[1], J Gonnissen[1], G T Martinez[1], A Béché[1], K E MacArthur[2], L Jones[2], P D Nellist[2] and S Van Aert [1]**

[1] Electron Microscopy for Materials Science (EMAT), University of Antwerp, Groenenborgerlaan 171, B-2020 Antwerp, Belgium
[2] Department of Materials, Uni versity of Oxford, 16 Parks Road, Oxford OX1 3PH, UK

E-mail: annick.debacker@uantwerpen.be

**Abstract.** Quantitative atomic resolution annular dark field scanning transmission electron microscopy (ADF STEM) has become a powerful technique for nanoparticle atom-counting. However, a lot of nanoparticles provide a severe characterisation challenge because of their limited size and beam sensitivity. Therefore, quantitative ADF STEM may greatly benefit from statistical detection theory in order to optimise the instrumental microscope settings such that the incoming electron dose can be kept as low as possible whilst still retaining single-atom precision. The principles of detection theory are used to quantify the probability of error for atom-counting. This enables us to decide between different image performance measures and to optimise the experimental detector settings for atom-counting in ADF STEM in an objective manner. To demonstrate this, ADF STEM imaging of an industrial catalyst has been conducted using the near-optimal detector settings. For this experiment, we discussed the limits for atom-counting diagnosed by combining a thorough statistical method and detailed image simulations.

## 1. Introduction

The observed intensity in atomic resolution STEM images is highly sensitive to the number of projected atoms in each atomic column. Therefore, quantitative ADF STEM has become a popular technique for nanoparticle atom-counting. In existing atom-counting methods the number of atoms is estimated from an ADF STEM image by a comparison with detailed image simulations or by using advanced statistical methods [1–4]. By analysing the total fraction of scattered electrons from each atomic column, the so-called scattering cross-section, it has been shown that the number of atoms in a single-element column can be counted with single-atom sensitivity on model systems, which are relatively stable under the incoming electron beam [2–5]. Here we discuss how we can extend this technique to count the number or atoms in more challenging nanostructures.

## 2. Statistical detection theory

In order to keep the incoming electron dose as low as possible but still retain single-atom precision, statistical detection theory can be used to optimise the instrumental microscope settings [6]. Similar to the use of statistical parameter estimation theory to quantify the precision

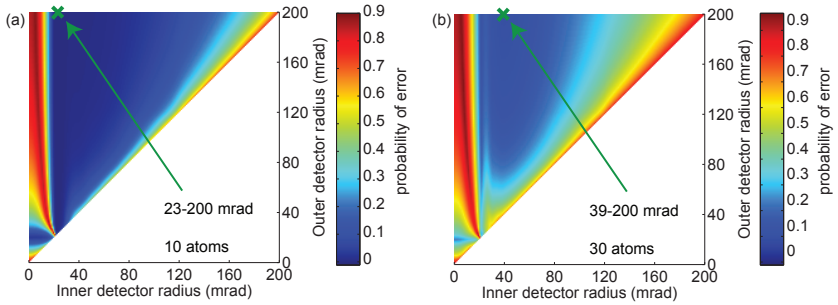


**Figure 1.** Probability of error as a function of inner and outer detector angle for Pt along the [110] zone axis for an electron dose of $10^4$ $e^-/Å^2$. (a) Probability of error for counting up to 10 atoms. (b) Probability of error for counting up to 30 atoms.

with which atom column can be located [7–10], the principles of detection theory allow one to quantify the probability of error for atom-counting [11]. This probability of error has been used to compare different image performance measures that can be used for atom-counting. Such analysis suggests that the scattering cross-sections perform equally well as the image intensities on a pixel by pixel basis and prove more robust than peak intensities. Moreover, based on an expression for the probability of error, it can be shown that for very thin objects low angle ADF STEM is optimal and that for thicker objects the optimal inner angle increases as illustrated in Fig. 1 [11].

## 3. Atom-counting on a Pt/Ir particle

Next, atom-counting will be demonstrated on an industrial bimetallic catalyst. Four images of the same Pt/Ir particle were recorded at different magnifications and electron doses under near-optimal detector settings (i.e. 35-190 mrad) at the QuAntEM, a double corrected FEI Titan$^3$ working at 300 kV with a 20.2 mrad semi-convergence angle. Because of their beam sensitivity and limited size, these particles provide a severe characterisation challenge, even under the optimal detector settings [12]. By combining simulation- and statistics-based methods, being completely independent of each other, the effect of dose and limited particle size on the reliability of atom-counting can be determined. In order to allow comparison with simulations, the images were normalised with respect to the incoming electron beam intensity [13]. Next, using statistical parameter estimation theory, the scattering cross-sections were quantified atomic column - by - atomic column. For this Pt/Ir particle, both atomic species ($Z_{Ir}$=77 and $Z_{Pt}$=78) have been treated in the same way, since the scattering cross-sections of Pt cannot be distinguished from the scattering cross-sections of Ir up to 30 atoms. An example analysis for the image recorded at the highest magnification (pixel size of 0.12 Å) and electron dose ($5.2 \times 10^5$ $e^-/Å^2$) is illustrated in Fig. 2; the scattering cross-sections are visualised in a histogram. The number of significant components and their scattering cross-sections were determined by evaluating the so-called integrated classification likelihood (ICL) criterion in combination with Gaussian mixture model estimation. These results allow us to quantify the number of atoms in each atomic column.
In Fig. 3, the experimental scattering cross-sections, i.e. the components of the Gaussian mixture model, resulting from the counting analyses are compared with the scattering cross-sections resulting from simulated images using STEMsim [14]. For image D (shown in Fig. 2(a)) with the highest magnification and electron dose, an excellent match was found. However, analysing images of lower magnification (less finely sampled image) and/or lower electron dose worsens the match with simulation. The same effect is observed when analysing a subsampled image, i.e. composed of every second pixel of image D, whereas the sampling has no effect on the reliability

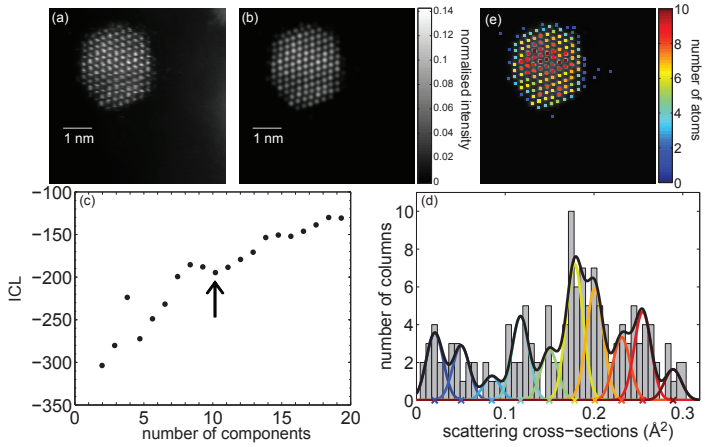


**Figure 2.** Illustration of the atom-counting procedure. (a) Experimental ADF STEM image. (b) Refined parametrised imaging model. (c) Evaluation of ICL as a function of the number of components. (d) Histogram of estimated scattering cross-sections together with the estimated Gaussian mixture model. (e) Quantification of the number of atoms in each atomic column.

as shown by the binned version of image D, i.e. by averaging the pixels. In the subsampled image, the lower dose of images A and B is mimicked. This leads to less precise measurements of the scattering cross-sections resulting in insufficient statistics for the determination of the number of components. However, when enhancing the statistics by combining the values of the scattering cross-sections of the four images collectively, the experimental values again match with simulated values. The study demonstrates that while the incoming electron dose is often lowered in order to reduce sample damage, the detected dose should be sufficiently large to retain single-atom precision, even when the image has been recorded under the optimal detector settings.

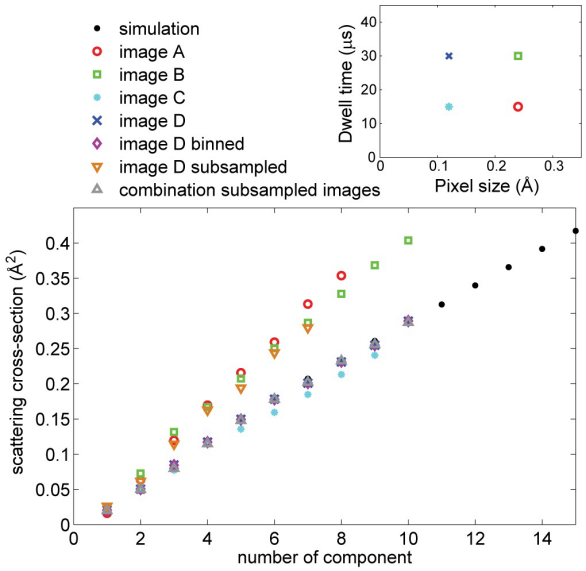


**Figure 3.** Comparison of experimental and simulated scattering cross-sections. The upper right graph shows the specific pixel size and dwell time for the individual images of the Pt/Ir particle.

## 4. Conclusions

In conclusion, using statistical detection theory, the detector settings can be optimised which becomes extremely important when looking at beam sensitive systems. A lower inner detector angle is suggested for thin objects in order to maximise the detected dose. This detector setting has been used for an atom-counting analysis of an industrial catalyst. It has been shown that even when employing optimal detector settings, a minimum level of electron dose is required to retain single-atom precision. The reliability of the atom-counting results could be studied by using a combination of advanced statistical methods and detailed image simulations [14].

## Acknowledgments

The authors acknowledge financial support from the Research Foundation Flanders (FWO, Belgium) through project funding (G.0368.15N, G.0369.15N, and G.0374.15N) and a PhD research grant to A De Backer. The research leading to these results has received funding from the European Union Seventh Framework Programme under Grant Agreement 312483 - ESTEEM2 (Integrated Infrastructure Initiative-I3), ERC Starting Grant 278510 Vortex, and the UK Engineering and Physical Sciences Research Council (EP/K032518/1). The authors acknowledge Johnson-Matthey for providing the sample and PhD funding to K E MacArthur. A Rosenauer is acknowledged for providing the STEMsim program.

## References

[1] LeBeau J M, Findlay S D, Allen L J and Stemmer S 2010 *Nano Letters* **10** 4405–4408

[2] Van Aert S, Batenburg K J, Rossell M D, Erni R and Van Tendeloo G 2011 *Nature* **470** 374–377

[3] Van Aert S, De Backer A, Martinez G T, Goris B, Bals S and Van Tendeloo G 2013 *Physical Review B* **87**

[4] De Backer A, Martinez G T, Rosenauer A and Van Aert S 2013 *Ultramicroscopy* **134** 23–33

[5] E H, MacArthur K E, Pennycook T J, Okunishi E, D'Alfonso A J, Lugg N R, Allen L J and Nellist P D 2013 *Ultramicroscopy* **133** 109–119

[6] Kay S M 2009 *Fundamentals of Statistical Signal Processing: Volume II Detection Theory* (New Jersey: Prentice-Hall, Inc.)

[7] den Dekker A J, Van Aert S, Van Dyck D, van den Bos A and Geuens P 2001 *Ultramicroscopy* **89** 275–290

[8] Van Aert S, den Dekker A J, Van Dyck D and van den Bos A 2002 *Journal of Structural Biology* **138** 21–33

[9] De Backer A, Van Aert S and Van Dyck D 2011 *Ultramicroscopy* **111** 1475–1482

[10] den Dekker A J, Gonnissen J, De Backer A, Sijbers J and Van Aert S 2013 *Ultramicroscopy* **134** 34–43

[11] De Backer A, De wael A, Gonnissen J and Van Aert S 2015 *Ultramicroscopy* **151** 46–55

[12] De Backer A, Martinez G T, MacArthur K E, Jones L, Béché A, Nellist P D and Van Aert S 2015 *Ultramicroscopy* **151** 56–61

[13] Rosenauer A, Gries K, Müller K, Pretorius A, Schowalter M, Avramescu A, Engl K and Lutgen S 2009 *Ultramicroscopy* **109** 1171–1182

[14] Rosenauer A and Schowalter M 2008 Stemsim - a new software tool for simulation of STEM HAADF Z-contrast imaging *Microscopy of Semiconducting Materials 2007* (*Springer Proceedings in Physics* vol 120) ed Cullis A and Midgley P (Springer Netherlands) pp 170–172